Reductive Preparation of Carbyne with High Yield. An *in Situ* Raman Scattering Study

J. Kastner and H. Kuzmany*

Institute of Solid State Physics, University of Vienna and Ludwig Boltzmann Institute of Solid State Physics, Strudlhofgasse 4, A-1090 Vienna, Austria

L. Kavan and F. P. Dousek

J. Heyrovský Institute of Physical Chemistry and Electrochemistry, Academy of Sciences of the Czech Republic, Dolejškova 3, CZ-18223 Prague 8, Czech Republic

J. Kürti

Department of Atomic Physics, R. Eötvös University, Puskin u. 5-7, H-1088 Budapest, Hungary

Received July 7, 1994; Revised Manuscript Received October 11, 1994®

ABSTRACT: Electrochemical reductive carbonization of poly(tetrafluoroethylene) with alkali metal (Li, Na, K) amalgams leads to a polymeric carbon with a partly carbynoid structure. Raman spectra measured *in situ* exhibited a strong line at around 2000 cm^{-1} which was interpreted as the C≡C−C stretching mode of a linear carbon chain with alternating carbon−carbon triple and single bonds (polyyne). The intensity and position of this line evidence an unusually high triple bond carbon content in our materials, which leads to relatively large conjugation lengths in the polyyne chains. The triple bond line shifts to higher wavenumbers with increasing laser energy; this can be elucidated in terms of the conjugation length model. A quantum chemical calculation for transition energies and matrix elements of oligoynes with different chain lengths is presented. In addition, the frequency of the Σ_g mode as a function of chain length is calculated. The conjugation lengths found correspond to 8−14 C atoms in the polyyne chain and increase with increasing atomic number of the alkali metal. The yield of polyyne and its stability against interchain cross-linking increase similarly. This supports our previous conclusions about the polyyne stability which were formulated on the basis of electronic conductivity and UV−vis spectra.

I. Introduction

In spite of the fascinating impact of fullerenes to carbon science, there still remain all-carbon molecules and solids about which we know almost nothing. They bring, however, at least theoretically a very unusual "linear dimension" (sp hybridization) into the structure of elemental carbon. All common carbon polymorphs (graphite, fullerenes, diamond, and lonsdaleite (=hexagonal diamond)) are virtually cyclic, composed from condensed six- and five-membered rings with sp^2- or sp^3-hybridized C atoms.[1] A linear modification of elemental carbon (carbyne) containing solely the chains of sp-hybridized C atoms has occasionally been mentioned in the literature[1,2] while seven solid carbyne polymorphs were characterized crystallographically.[1] These results were, however, also subjected to strong criticism, up to a complete rejection of the carbyne concept.[3] Although this extreme opinion is not shared by the majority of other authors,[1,2] we have to admit that the carbyne history still remains one of the most contradictory and confusing topics in carbon science.

A complete X-ray diffraction analysis of any carbynoid species confirming the chain structure is not yet available due to the lack of a suitably sized carbyne single crystal. Therefore structural models of carbyne are supported only by indirect experiments such as electron diffraction of "oriented carbyne layers"[2] or by theoretical considerations.[4−9] A linear polymeric sp-hybridized carbon molecule can be derived either from a chain with alternating single and triple bonds, i.e., polyyne (polyethynylene):

$$-C\equiv C-C\equiv C-$$

with calculated bond lengths 120.7 and 137.9 pm[1] or alternatively from a less stable chain of only double bonds (128.2 pm), i.e., polycumulene (polyethylenediylidene):[1]

$$=C=C=C=C=$$

The polyyne configuration is preferred energetically to the cumulene one because of a stabilization by the Peierls distortion.[4,5,7,8] Calculated Peierls gaps are in the range between 2 and 5 eV.[7,8] In this sense polyyne is a conjugated polymer with two π-electrons per carbon atom on the backbone. Thus, it can be expected that models appropriate for sp^2-conjugated polymers are applicable here as well.

In contrast to infinite carbon chains, small C_n molecules ($n \leq 8$) tend to exhibit a cumulene-like structure with only a slight bond alternation.[10] For n even C_n molecules two ground state structures are very close in energy and may coexist: a linear and a cyclic (rhombic) structure.[10,11] C_3 and other small C_n molecules ($n \cong 4-10$), as well as oligoynes (H−(C≡C)$_n$−H) are presumably linear.[10,12]

The occurrence of natural carbynes has been mostly reported in rather exotic environments such as interstellar space, meteorites, and meteoritic craters.[1] Synthetic routes to carbynes include oxidative dehydropolymerization of acetylene catalyzed with Cu^{2+} ions, condensation of carbon vapor or liquid carbon, phase transitions of diamond or graphite, and shock compression of glassy carbon.[1] Occurrence of carbynes was reported also in the products of dehydrohalogenation of poly(vinylidene halides)[3,13,14] and chlorinated polyacetylene[15] in alkaline medium.

® Abstract published in *Advance ACS Abstracts,* December 1, 1994.

0024-9297/95/2228-0344$09.00/0

Another synthetic strategy to carbynes consists in a complete reductive dehalogenation of perhalogenated (macro)molecules. This reaction proceeds at room temperature by action of some anion radicals, alkali metals, and alkali metal amalgams or electrochemically at a Pt cathode in aprotic electrolyte solutions (for a review, see ref 16). The most carefully studied perhalogenated precursor is poly(tetrafluoroethylene) (PTFE).[16-24] The reaction of PTFE and other perhalogenated molecules with alkali metal amalgams is, however, also "electrochemical" in nature since it is controlled by a spontaneous discharge of an *in situ* formed galvanic cell with an amalgam anode and continuously renewed carbon cathode.[16,22] Hence we have introduced the term "electrochemical carbon", which is equally usable for the products of cathodic as well as amalgam reduction of perhalogenated (macro)molecules.[16]

There has been a long-term discussion about the occurrence of carbyne in (electrochemical) carbons obtained by reductive defluorination of PTFE.[9,16,21-24] This reasoning follows from the fact that the conformation of the starting linear fluorocarbon chain may remain intact under the moderate conditions of electrochemical reductive carbonization. Thus, the formation of "electrochemical carbyne" can schematically be depicted as follows:

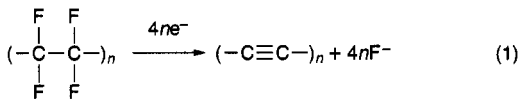

$$(-\underset{F}{\overset{F}{C}}-\underset{F}{\overset{F}{C}}-)_n \xrightarrow{4ne^-} (-C\equiv C-)_n + 4nF^- \qquad (1)$$

We shall further denote the reaction product as C–MeF (Me stands for a cation of the supporting electrolyte, i.e., alkali metal in the case of the reduction by amalgams). The reaction byproduct, i.e., alkali metal fluoride (MeF), forms nanosized crystallites interspersed between the nascent carbyne chains. These crystallites are assumed to preserve sterically to some extent the naked carbyne chains against cross-linking and chemical decomposition in a reactive environment.[16,21,23] The former reaction leads to a graphite-like (graphene) species.[21,23]

There are so far only indirect supports for this preconception; they were formulated on the basis of X-ray diffraction,[24] electronic conductivity,[23] UV–vis spectra,[21] and some other considerations.[19,21] For instance, the radial electron density distribution curve, determined by X-ray diffraction analysis of C–LiF, indicates the average carbon–carbon distance $\delta_{CC} = 135 \pm 4$ pm, which was interpreted as a superposition of graphitic (sp^2, $\delta_{CC} = 142$ pm, 70–45%), diamond-like (sp^3, $\delta_{CC} = 154$ pm, 0–15%), and also carbynoid (sp, $\delta_{CC} \cong 120$ pm, 30–40%) structures.[24] The same picture follows also from the solid-state ^{13}C-NMR study, which indicates the presence of sp, sp^2, and sp^3 carbon atoms in the product of the PTFE reduction with benzoin dianion.[17]

Carbynes (polyynes) are further characterized by IR spectroscopy, especially by the C≡C stretching mode ($\nu_{C\equiv C}$)[13-15,21] at 2100–2200 cm^{-1}. Infrared spectra of carbons prepared by reductive defluorination of PTFE were studied in several papers,[16-18,21] but the mentioned carbyne line is detectable only when the contact of samples with air oxygen and humidity is excluded.[21] The C≡C stretching mode was also detected in the products of dehydrohalogenation of chlorinated polyacetylene[15] and poly(vinylidene fluoride).[13,14,25,26] In the first case, a formation of polyyne was considered[15] but in the latter case, polycumulene[13] or a mixture of polycumulene and polyyne linkages were found.[13,25,26]

The C≡C stretching mode of polyyne at 2100–2150 cm^{-1} is also detectable by Raman spectroscopy. This was first reported in 1974 by Nakamizo et al.[27] for carbyne ("white carbon") samples prepared from natural graphite by CO_2-laser treatment or by sputtering with a ruby laser. Both the irradiated graphite and sputtered carbon deposit show a new feature at 2140 cm^{-1} in addition to the usual Raman peaks at 1580 and 1360 cm^{-1}. The peaks at 1580 and 1360 cm^{-1} (also called G and D peaks) are regularly observed in polycrystalline carbons such as carbon black, glassy carbon, coal, pyrolytic carbon, carbon fibers, etc.[28] The appearance of a new Raman band at 2150 cm^{-1} was also observed in graphite samples after bombardment with energetic protons, deuterons, and helium ions (10–15 keV)[29] and in the carbonaceous materials prepared by the reduction of PTFE with radical anions.[17,18] In the latter case, the bands at 2176 and 2239 cm^{-1} were assigned to the C≡C stretching mode (and combination bands with other C–C stretching modes), but the exact structural interpretation is controversial. Nishihara et al.[30] have interpreted the Raman spectrum of "electrochemical carbon" made by cathodic reduction of perhalogenated butadiene as that of graphite, while no carbyne Raman bands were reported.

The best resolved Raman spectra of carbyne were obtained with the products of dehydrochlorination of chlorinated polyacetylene[15] and poly(vinylidene chloride).[31] In the first case, Akagi et al.[15] have supposed solely the polyyne structure with only one carbyne line at around 2150 cm^{-1}. The two additional lines at 1140 and 1550 cm^{-1} in the Raman spectrum were assigned to *trans*-polyacetylene present in their samples due to an unperfect chlorination. The carbyne line at 2150 cm^{-1} was interpreted as the C≡C stretching mode of polyyne. This line exhibited an upshift with the energy of the exciting laser of about 60 cm^{-1}/eV.

The Raman spectrum of dehydrochlorinated poly(vinylidene chloride) studied by Berdyugin et al.[31] shows basically the same features, i.e., two distinct peaks at 1550 and 2150 cm^{-1}; it was interpreted solely in terms of the polycumulene structure,[31] which was supported by the analogy with the Raman spectrum of poly(diacetylene) (1520 and 2120 cm^{-1}). This is, however, a rather vague argument for polycumulene, since poly(diacetylene) may in principle exhibit both the acetylenic and the butatrienic structures:

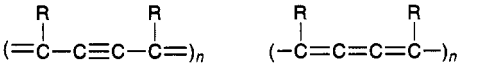

$$(=\underset{R}{\overset{R}{C}}-C\equiv C-\underset{R}{\overset{R}{C}}=)_n \qquad (-\underset{R}{\overset{R}{C}}=C=C=\underset{R}{\overset{R}{C}}-)_n$$

The first isomer is, moreover, considered more stable for most R (including H) at normal conditions.[6]

This paper discusses the Raman spectra of carbynoid species prepared by reaction of alkali metal amalgams with poly(tetrafluoroethylene) (PTFE) and poly(tetrafluoroethylene-*co*-hexafluoropropene) (FEP). The mentioned preparative method of carbon from fluoropolymers is superior to the electrochemical reduction of fluoropolymers on metal electrodes or by various chemical agents since the reaction course and its product are best defined.[16] Since the experimental results exhibited an unusually large amount of carbon–carbon triple bonds, our materials will be termed "carbynes" independent of whether or not there is enough evidence for an ideal linear carbyne chain. For the evaluation of

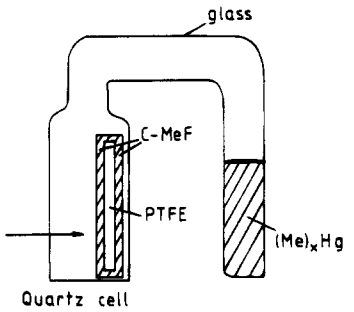

Figure 1. Optical quartz cell used for *in situ* measurements. For the preparation of the carbyne layer the alkali metal amalgam was contacted with the fluoropolymer.

experimental data an effective linear chain model will be assumed.

II. Experimental Section

PTFE foils (6.4, 20, 60, and 100 μm thick) and FEP foils (50 μm thick) containing 20 mol % of hexafluoropropene units were purchased from ICI (U.K.) and from Asahi Chemical, respectively. Carbonized layers on PTFE and FEP were prepared by reaction of the outgassed fluoropolymer foils with liquid alkali metal amalgam in vacuum. The amalgam concentrations were in the range 0.9–1.2 atom %. The amalgam preparation, purification, chemical analysis, and other experimental details are described elsewhere.[22]

Transmission UV–vis measurements were performed *in situ* using evacuated quartz optical cells and a Zeiss M40 or a Hewlett-Packard 8452A spectrometer. A schematic drawing of the optical cell used is shown in Figure 1. The sample preparation and measurement of spectra proceeded as follows: First the cell transmission background with intact PTFE or FEP foil was determined. (The use of FEP is superior to PTFE due to the higher optical transparency of a blank fluoropolymer foil.) Subsequently the optical cell was filled with liquid $(Me)_xHg$ from the side ampule, and the reaction proceeded for a desired time at 25 °C, producing a thin C–MeF film on top of the fluoropolymer foil. Finally, the transmission spectrum was recorded after decanting the amalgam back into the side ampule, while care was taken that no amalgam droplets remained on the sample surface. The preparation/measurement cycles were repeated several times, and the obtained spectra were normalized by subtracting the absorbance of the unreacted fluoropolymer foil and the cell background. The absorbance values found were eventually divided by 2 to compensate the fact that the reaction produces a double-sided carbonized foil. The subtractively normalized spectra of C–MeF did not show considerable differences if a thin PTFE foil was used instead of FEP. We present further on only the spectra of carbonized FEP, which showed a lower optical background.

The preparation of samples for Raman studies proceeded essentially in the same way as mentioned above while an analogous apparatus with an evacuated quartz cell was used. The C–MeF layers for Raman studies were prepared at 20–23 °C exclusively from PTFE as a precursor. The reaction times were 5 min (Li), 3 h (Na), and 35 days (K) which corresponds[16,22] to the thicknesses of carbonized PTFE layers 820 (Li), 280 (Na), and 170 nm (K). These layer thicknesses were chosen as the best compromise between the necessary optical absorbance and Raman intensity and a reasonably short reaction time. Thus, Raman spectra obtained contained prevailingly the signal from the C–MeF layer. The slight contribution from the PTFE support (narrow lines at 385, 730, and 1380 cm^{-1}) does not interfere with the assignment of the C–MeF spectrum.

The Dilor XY multichannel spectrometer with a liquid N_2-cooled CCD detector was used to measure spectra after excitation with lines from an Ar^+ and a Kr^+ laser with wavelengths ranging from 406 up to 676 nm. Measurements were taken in backscattering geometry and with a typical laser power of 0.5–1 mW. This laser power was low enough so that the Raman spectra did not change with time of exposure. The spectral resolution was between 5 cm^{-1} (for excitation with 676 nm) and 10 cm^{-1} (for excitation with 406 nm). A typical accumulation time was 10 min. The spectra of freshly prepared samples exhibited a luminescence background, which bleached with ageing (cf. Figure 4). For the presentation, a linear background was subtracted from the Raman spectra.

For measurements in the whole frequency range 200–2200 cm^{-1}, it was necessary to add consecutive spectral ranges, which introduced slight discontinuities (humps) at the overlap. These humps appear in all Raman spectra recorded with multichannel detectors. Since normally the investigated Raman lines are much narrower than the instrumental spectral range, these humps do not cause any problems. In our case the Raman lines are, however, very broad so that a careful adjustment was necessary to minimize the spectrometer-induced discontinuities, and the spectral ranges were selected to match the regions of individual Raman lines in an optimum way.

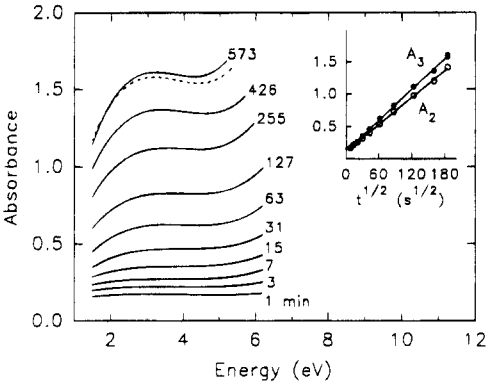

Figure 2. UV–vis spectra of the C–NaF layers prepared by the reaction of FEP foil (50 μm thick) with Na amalgam at 25 °C. The reaction time (in minutes) is indicated. The absorbance of the unreacted FEP support was subtracted. Dashed curve: the spectrum for a reaction time of 573 min; measured after 10 h. The inset shows the plot of the C–NaF absorbance at 2 eV (A_2) and 3 eV (A_3) vs the square root of the reaction time.

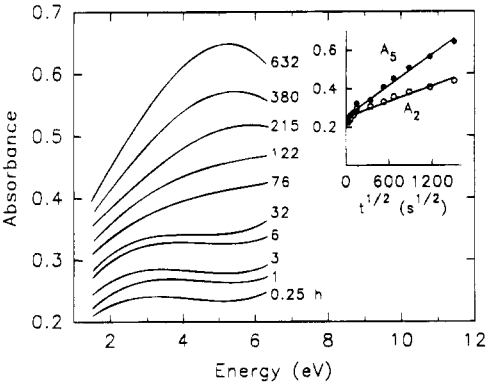

Figure 3. UV–vis spectra of the C–KF layers prepared by the reaction of FEP foil (50 μm thick) with K amalgam at 25 °C. The reaction time (in hours) is indicated. The absorbance of the unreacted FEP support was subtracted. The inset shows the plot of the C–KF absorbance at 2 eV (A_2) and 5 eV (A_5) vs the square root of the reaction time.

III. Results

A. UV–vis Absorption Spectroscopy. UV–vis spectra of the FEP-supported C–NaF and C–KF layers are shown in Figures 2 and 3. (For comparison with C–LiF, see ref 21). To minimize the effects of sample ageing, the spectra were measured immediately after preparation. The ageing is demonstrated by a dashed curve in Figure 2 and can be attributed to slow carbyne-

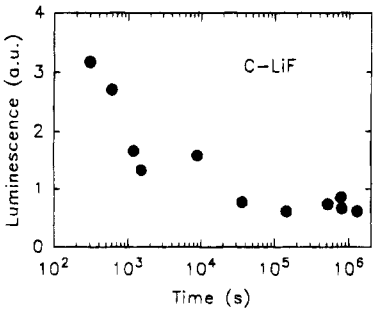

Figure 4. Luminescence background at 2300 cm^{-1} of C–LiF after excitation with 457 nm as a function of time elapsed after the preparation started.

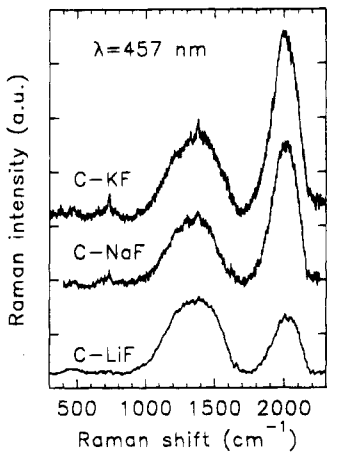

Figure 5. Raman spectra of C–LiF, C–NaF, and C–KF as excited with 457 nm.

to-graphene cross-linking.[16,21,23] The changes in absorbance accompanying this process are dependent on Me and wavenumber while an "isosbestic point" appears around 2 eV both for C–NaF and C–LiF (cf. Figure 2 and ref 21). Insets in Figures 2 and 3 show the dependence of absorbances values vs the square root of the preparation time.

B. Raman Scattering. Laser excitation of the C–MeF samples was always accompanied by a broadband luminescence which bleached with time of ageing as shown in Figure 4 for C–LiF. This luminescence can be attributed to radicals, since radicals are known to act as recombination centers. These radicals are formed during the carbonization process[16,19] and are neutralized with the ageing of the carbonized layer.

Figure 5 shows Raman spectra of thin C–LiF, C–NaF, and C–KF layers prepared on top of a PTFE foil. In order to have comparable ageing times, the spectra presented in Figure 5 were measured about 40 days after the start of the preparation. There are two dominating lines, one asymmetrically broadened between 1000 and 1600 cm^{-1} and a second one around 2000 cm^{-1}. The former line is common for all forms of polycrystalline graphite or "amorphous carbon" with a broad distribution of sp^3- and sp^2-bonded carbon atoms;[32] it will further be referred to as a line of "amorphous carbon" (a-C). The second line occurs in the region of the C–C stretching mode of sp-bonded carbon; for simplicity, it will further be referred to as the "carbyne line". Compared to the a-C line the relative intensity of the carbyne line increases and the Raman shift decreases when the alkali metal is varied from Li to Na and K. This behavior is illustrated in Table 1, where the results are summarized. For comparison the molar volume (V_m) and the lattice constant (a) of the corresponding alkali metal fluorides are included.

Table 1. Position of the Carbyne Line and Relative Intensity of This Line to the a-C Line for C–MeF (Me = Li, Na, and K) in Comparison with the Molar Volume (V_m) and the Lattice Constant (a) for the Corresponding MeF[a]

composite	$\nu_{carbyne}$ (cm^{-1})	$I_{carbyne}/I_{a\text{-}C}$	V_m (cm^3/mol)	a (Å)
C–LiF	2042 ± 5	0.55 ± 0.2	9.8	4.03
C–NaF	2006 ± 4	1.6 ± 0.2	14.9	4.62
C–KF	2002 ± 4	2.0 ± 0.2	23.2	5.34

[a] The wavelength of the exciting laser line was 457 nm.

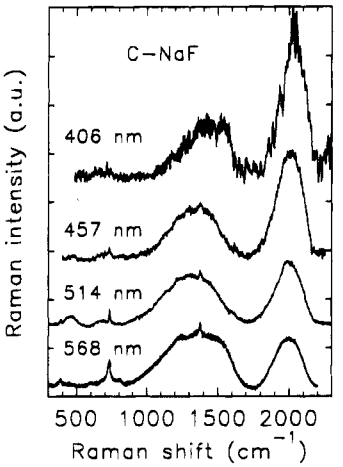

Figure 6. Raman spectra of C–NaF as excited with different laser lines (568, 514, 457, and 406 nm). The spectra were normalized so that the a-C lines have equal intensities in all cases.

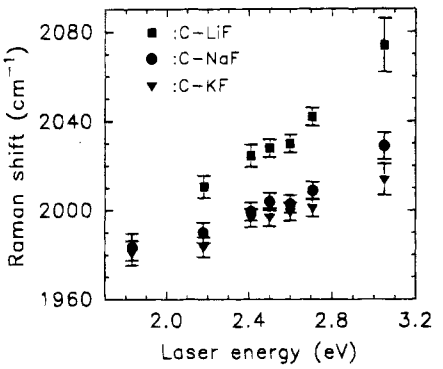

Figure 7. Raman shift of the line for the carbyne mode versus the exciting laser energy for C–LiF (boxes), C–NaF (circles), and C–KF (triangles).

In addition to the dominating features in the Raman spectrum, there are two broad and weak lines around 420 and 700 cm^{-1}, which were also observed in glassy carbon and different forms of amorphous carbon.[33,34] The narrow lines at 285, 730, and 1380 cm^{-1} originate from PTFE.

In Figure 6 Raman spectra of C–NaF for different laser excitations are shown. The spectra were normalized to equal intensities for all a-C lines. An increase of the energy of the exciting laser leads to an increase of the Raman intensity and to an upshift of the carbyne line. The change of the peak position of the carbyne line as a function of the laser energy is plotted in Figure 7. For all samples the position of the carbyne line shifts almost linearly to higher wavenumbers with increasing energy; this dispersion effect is much more pronounced for C–LiF (73 cm^{-1}/eV) as compared to C–NaF (39 cm^{-1}/eV) and C–KF (31 cm^{-1}/eV). The dispersion effect

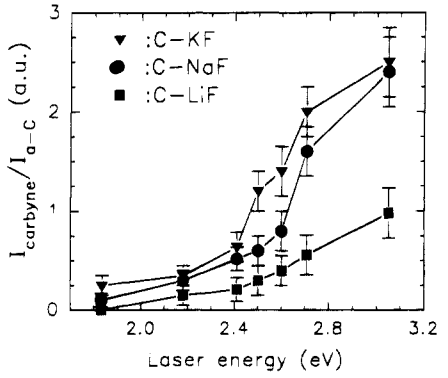

Figure 8. Intensity ratio of the line for the carbyne mode to the line of amorphous carbon versus the energy of the exciting laser for C−LiF (boxes), C−NaF (circles), and C−KF (triangles).

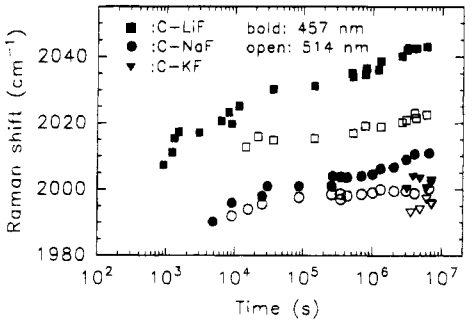

Figure 9. Raman shift of the carbyne line as a function of time after the preparation for C−LiF (boxes), C−NaF (circles), and C−KF (triangles) was started, as measured with 514 (open) and 457 nm (bold).

is well known from conjugated polymers for the C=C double bond stretching mode. It can be explained by a photoselective resonance excitation of different segments of the polymer.[34,35] A similar model might be applicable to the carbyne mode.

The intensity ratio of the carbyne line and the line of a-C between 1000 and 1600 cm^{-1} versus the energy of the exciting laser is plotted in Figure 8. The ratio increases with increasing laser energy and approaches a maximum somewhere above 3 eV. A plot of the intensity ratio of the carbyne line to the line for PTFE at 730 cm^{-1} exhibits essentially the same behavior.

Due to their high π-electron density carbynes are very reactive and normally decompose even in vacuum.[16] To investigate the stability of the carbyne present in our samples, we studied the change of the Raman spectra with time. Figure 9 shows the Raman shift of the carbyne line as a function of time after starting the preparation. The spectra were taken immediately after the carbonization was finished. The maximum of the carbyne line is apparently upshifting with time. This ageing process is faster for C−LiF than for C−NaF and C−KF since the rate of upshift of the carbyne line decreases in this series (see Figure 9). The ageing process mainly affects the position of the carbyne line. The time-dependent decrease of the relative intensity of the carbyne line to the a-C line is less pronounced. A significant decrease is only observed after several weeks of ageing.

IV. Calculation of Electronic and Vibrational Structure

A. Electronic Structure. To interpret the experimental spectra a linear chain model was assumed and the electronic and vibrational structure was calculated using a Longuet-Higgins−Salem (LHS) type model Hamiltonian[36] for strictly linear oligoynes with various lengths. These calculations are similar to previous work reported for finite oligoenes[37] but two independent electronic subsystems had to be considered for the oligoynes.

The LHS model treats the π-electrons within the Hückel scheme but considers also the σ-electrons by an effective potential. This allows a self-consistent optimization of the geometry (bond lengths) using the empirical relationship between a bond length and the corresponding bond order. We summarize the most essential points of the LHS model for oligoynes; a detailed description for a linear chain and for the general case can be found in refs 37 and 38.

The Hamiltonian of the system can be written as

$$\hat{H} = \hat{H}_\pi + \hat{H}_\sigma \tag{2}$$

where the Hamiltonian of the π-electrons in the second quantized formalism is

$$\hat{H}_\pi = \sum_{i,s,t} \beta(r_i)(a^+_{ist}a_{i+1,st} + a^+_{i+1,st}a_{ist}) \tag{3}$$

In eq 3 a^+_{ist} and a_{ist} are the creation and annihilation operators for the atomic orbitals characterized by $\{ist\}$. i runs from 1 to $N-1$ (N is the even number of C atoms in the chain), s denotes the spin, and t accounts for the two independent π-systems, r_i is the length of the bond formed by atoms i and $i+1$, $\beta(r_i)$ is the corresponding resonance integral, which is assumed to have an exponential dependence on bond length:

$$\beta(r_k) = -Ae^{-(r_k/B)} \tag{4}$$

The Hamiltonian of the σ-electrons is

$$\hat{H}_\sigma = \sum_k^{N-1} f_\sigma(r_k) \tag{5}$$

where the summation runs over all bonds. The diagonalization of $\hat{H}_\pi$ is performed iteratively until Coulson's linear relationship

$$r_k = R_0 - \kappa p_k \tag{6}$$

between bond length (r_k) and mobile bond order (p_k) is fulfilled for all bonds. A, B, R_0, and κ are well-known LHS parameters for carbon π-bonds. It can be shown that this is equivalent to choosing the σ-potential for the individual bonds as

$$f_\sigma(r) = \frac{2}{\kappa}\beta(r)(r - R_0 + B) \tag{7}$$

The bond orders can be expressed by the linear combination factors of the atomic orbitals for the occupied molecular orbitals. For the same geometry the mobile bond orders for oligoynes are exactly 2 times the one for the oligoenes. Therefore, the relaxation process using eq 6 leads to different geometries and so to different electronic properties, even in the case of the same LHS parameters A, B, R_0, and κ are used for oligoynes and oligoenes. In fact, the bond length−bond order relationship is not linear for the whole region from $p = 0$ to $p = 2$. A quadratic (or higher) dependence, however, would lead to even qualitatively incorrect f_σ;

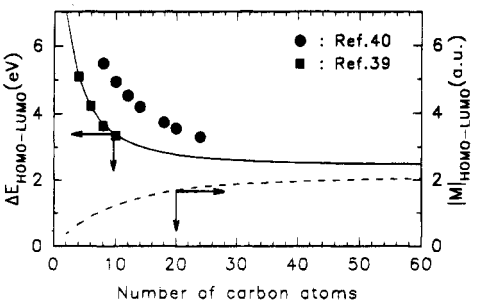

Figure 10. Calculated (line) and experimental (symbols) transition energies as well as transition-matrix elements (dashed line) for the HOMO–LUMO transition as a function of the number of carbon atoms of oligoynes. The experimental HOMO–LUMO transition energies were obtained by optical absorption spectroscopy on acetylenes (circles, ref 40; boxes, ref 39).

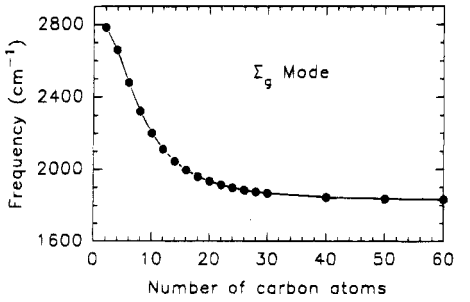

Figure 11. Frequency of the Σ_g ("k = 0") mode of oligoynes as a function of the number of carbon atoms, calculated by the LHS model. For $N = \infty$ this mode corresponds to the optical mode of polyyne.

therefore we still used a linear relationship, but with parameters which are adequate for p between 2 and 1 rather than for p between 1 and 0. These parameters are therefore different from those used in refs 37 and 38: $R_0 = 1.46$ Å instead of 1.54 Å and $\kappa = 0.13$ instead of 0.21. Because in the present problem only one kind of atoms with π-electrons is considered, all energies (π and σ as well) scale with A in eq 4. With $A = 170.4$ eV instead of 243.5 eV used in refs 37 and 38, the calculated HOMO–LUMO (highest occupied molecular orbital–lowest unoccupied molecular orbital) transition energies are in good agreement with the experimental values of Kloster-Jensen[39] as can be seen in Figure 10. The values reported by Eastmond et al.[40] which are included as well are too high. The dipole matrix elements for HOMO–LUMO transition are also shown in Figure 10. They will be used for the evaluation of the experimental data.

B. Vibrational Structure. The normal coordinate analysis for the stretching modes of oligoynes with various chain lengths was carried out by Wilson's well-known GF formalism, similarly to the case of oligoenes.[37] The force constant matrix was obtained from numerical derivation of the total ($\sigma + \pi$) energy as calculated by the LHS model, with respect to the various bond length. For a strictly one-dimensional chain consisting of N (N even) identical atoms there are $N/2$ Σ_g modes which are Raman active. For $N \rightarrow \infty$ only the $k = 0$ mode remains Raman active. This mode is equivalent to the special mode in finite oligomers where the neighboring carbon atoms vibrate in opposite phase. The amplitude of the mode in the oligomers is more or less uniform in the center part for long enough molecules and decreases at the ends. Figure 11 shows the calculated vibrational frequencies for the Σ_g "$k = 0$" modes of oligoynes with various lengths. The frequency decreases with increasing number of carbon atoms.

V. Discussion

A. UV–vis Absorption Spectroscopy. From the electrochemical model of the fluoropolymer–$(Me)_xHg$ reaction, it follows that the C–MeF layer thickness (L) is proportional to the square root of the preparation time (t).[16,22] The Lambert–Beer law gives the optical absorbance (A) as

$$A = \alpha L = \alpha a k t^{1/2} \tag{8}$$

where α is the absorption coefficient of the C–MeF composite. The constant a is a dimensionless expansion factor,[16,22] which amounts to 1.22, 1.88, and 2.56 for C–LiF, C–NaF, and C–KF,[41] respectively. k is a rate constant with a value of 47.0, 2.7, and 0.1 nm $s^{-1/2}$ for Me = Li, Na, and K,[16,41] respectively.

Insets in Figures 2 and 3 demonstrate that experimental absorbances are in accord with eq 8, except for the very beginning of the reaction (below ca. 1 min for C–NaF and 6 h for C–KF). A detailed discussion of this effect will be presented elsewhere.[41] From the slope of the linear parts of the A vs $t^{1/2}$ plots and eq 8, we can deduce the absorption coefficient α to be 1.6×10^4 cm^{-1} at 3 eV for C–NaF and to be 1.0×10^4 cm^{-1} at 5 eV for C–KF. Correction for the carbon concentration in C–MeF gives absorption coefficients within the range $(1.1–1.3) \times 10^5$ cm^{-1} in both cases, which is a typical value for amorphous carbon.[32] Figures 2 and 3 demonstrate that a reasonably linear Lambert–Beer plot can be obtained not only for absorbances at the isosbestic point (A_2) but also at other energies (A_3, A_5). This indicates that ageing plays a minor role at the experimental conditions used.

The optical absorption spectrum shows comparable features to those of other carbynoid materials, i.e., a broad band with an absorption edge in the red (near-infrared) region.[15,17,21,25] In the case of C–NaF and C–LiF[21] there is a broad band with a maximum at ≈3 eV. In C–KF this band can be only distinguished from the background within the first 32 h of the carbonization process. For longer reaction times the absorbance spectrum is dominated by a broad band with a maximum at ≈5 eV, but the band at ≈3 eV is probably still present.

As can be seen in Figure 8 the intensity ratio of the carbyne Raman line and the a-C line follows the absorption of all three composites. Thus, it is tempting to assume that this unknown absorption band at ≈3 eV corresponds to an intrinsic transition of the carbyne, probably to the HOMO–LUMO transition. The appearance of a broad but clear transition in the absorption spectrum supports the assumption that carbyne prefers the semiconducting polyyne configuration and not the metallic polycumulene structure. Considering that there are only finite carbon chains present in the samples, the position of the observed absorption band is in good agreement with calculations for infinite polyyne chains by Springborg et al.,[8] who reported a Peierls gap of ≈2 eV. The value of ≈5 eV for E_g calculated by Rice et al.[7] seems to be too high.

The absorption threshold shifts to lower energies as the C–MeF sample ages (cf. dashed curve in Figure 2), which is in qualitative accord with the predicted decrease of the optical band gap during the polyyne-to-graphene cross-linking. The interchain cross-linking

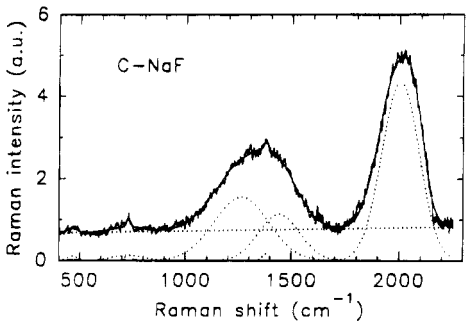

Figure 12. Raman spectrum of C–NaF after 457 nm excitation. Full lines are experimental data and dotted lines are the deconvoluted Raman lines.

causes reportedly the transition from the semiconductor- to a metal-like band structure.[9] A more detailed discussion of the C–MeF electronic spectra, including the ageing effects, will be presented in a subsequent publication.[41]

B. Raman Scattering. The Raman spectra of carbonized fluoropolymers show two distinct features. There is a broad asymmetric line between 1000 and 1600 cm^{-1}, which is characteristic for all forms of amorphous carbon, and a second line at higher wavenumbers. The a-C line can be deconvoluted into two Gaussian lines at around 1300 and 1500 cm^{-1}, which are designated in the literature as the D and G lines.[28,33] This is demonstrated in Figure 12. The G line is the broadening of the E_{2g} mode of crystalline graphite when the long-range order is lost. The D line is disorder induced. The ratio of the integrated intensity of the D line to the G line, $R = I_D/I_G$, depends inversely on the in-plane graphite crystallite size L.[32,42] The dependence of R on L holds over the extended range $0.001 < R < 1$ and $300 > L > 2.5$ nm. In our case $R = 1.8$, which is outside the valid range. This is an indication for strong disorder in the carbonized layer and for contributions to the Raman line between 1000 and 1600 cm^{-1} from sp^3-bonded atoms. Thus, the carbonized films must contain a broad distribution of sp^3 and sp^2 bondings and the sp^2-bonded graphite-like carbon clusters are smaller than 2.5 nm. This result compares well with X-ray diffraction studies by Červinka et al.,[24] who obtained a size of 0.6–1.6 nm for carbon clusters in the pure carbon phase from C–LiF.

The second strong line at around 2000 cm^{-1} is of considerable diagnostic significance because it may be assigned to the carbyne chains in our sample. It is important to notice that there is only one strong carbyne line present in the Raman spectrum. This is in contradiction to Berdyugin et al.,[31] who observed a second line of the carbyne at around 1550 cm^{-1}. One could argue that a weak line might be hidden under the a-C line in our case. If so, this line must be very weak; otherwise, it should be observable in C–NaF and C–KF after excitation with the blue laser, where the line around 2000 cm^{-1} is much stronger than the a-C line. Hence, we conclude that no additional carbyne line is present in the Raman spectrum of our material.

The two weak and broad lines in the low frequency spectrum at 420 and 700 cm^{-1} in Figure 5 probably originate from the a-C, since similar lines were also observed in glassy carbon and different forms of amorphous carbon.[33] These lines were explained by disorder-induced Raman scattering[33] and their positions coincide with maxima at the phonon density of states. The shape and position of these low-frequency lines depend on the preparation conditions[23] but are generally similar to those observed here.

More information can be drawn from the carbyne line at ≈2000 cm^{-1} by comparing the possible modes of the two carbyne modifications:

Polycumulene: A strictly linear polycumulene chain has only one atom per unit cell and can be regarded as a classical example for a linear chain, which has only one acoustical and no optical mode.

Polyyne: A strictly linear polyyne chain belongs to the $D_{\infty h}$-symmetry point group and has two atoms per unit cell. Due to its high symmetry and simplicity, it has only one Raman-active mode with Σ_g symmetry. This mode is the C≡C or more accurately the C≡C–C stretching mode, which has usually a frequency in the range from 1950 up to 2300 cm^{-1} depending on the force constants and neighboring bondings.

The interpretation of the Raman spectra of carbonized fluoropolymers in terms of a strictly linear polyyne seems to be more straightforward than in terms of a polycumulene. The only possibility to explain the observed Raman spectra with a cumulene configuration requires a zigzag structure. This was indeed suggested by Berdyugin et al.[31] Since a deviation from linearity for sp-bonded carbon atoms is energetically very unfavorable, this interpretation is not very likely. The energetic arguments are stronger for a polyyne structure, although it cannot be excluded that there are also some cumulene-like species present. Especially very short C_n molecules with $n \leq 8$ may exhibit a cumulene-like structure.[10] In general, we regard the appearance of only one carbyne line in the Raman spectrum as an experimental indication that the polyyne structure is energetically more stable than the polycumulene structure.

The maximum of the carbyne line is somewhat lower than the maxima of lines observed in acetylenes and in carbynoid samples as reported by Akagi et al.[15] and Berdyugin et al.[31] This difference might have two reasons:

1. The dependence of vibrational properties on the conjugation length is well known. Mode frequencies strongly increase when the conjugation length gets very short. Because of the low intensity of the C≡C triple bond stretching mode in the spectrum reported by Akagi et al. and Berdyugin et al., their samples contained only a small amount of carbyne with a rather low conjugation length.

2. There is some "superstoichiometric" alkali metal incorporated in the carbonized layers, which leads to a product with a typical composition C_5Me[16,22] where the carbon skeleton is reduced (n-doped). This would lead to a softening of the C≡C stretching mode analogously to the softening of the pentagonal pinch mode in doped C_{60}[43] because antibonding states become occupied.

Another important difference between the material of Akagi et al.[15] and Berdyugin et al.[31] as compared to the material used here originates from the different routes of preparation. Both groups used an organic reaction to prepare the carbyne. Thus, there might be always some byproducts like polyacetylene, acetylene oligomers, or other compounds which contribute to the Raman spectrum as well. Contrary to that, the route depicted here is well defined. There is no hydrogen present in the samples, just carbon and inorganic alkali fluorides, which have no Raman lines in the high-frequency region. Hence, the line at around 2000 cm^{-1} definitely originates from a pure carbon phase only.

As demonstrated in Figure 5 and Table 1, the intensity ratio of the carbyne line and the a-C line increases as Li is replaced by Na or K. This indicates that the amount of sp-bonded carbon atoms increases in the same direction. Moreover, the maximum of the carbyne line shifts to lower wavenumbers, which shows that also the region of noninterupted sp-bonded carbon chains (=conjugation length) increases in the same direction. It is interesting to compare the Raman results for C−MeF with physical data from the corresponding alkali metal fluorides. The molar volumes (V_m) and the lattice constants (a) for the latter are included in Table 1. Both V_m and a increase as the carbyne line shifts to lower wavenumbers and the relative intensity of the carbyne line compared to the a-C line increases. This behavior supports the suggested stabilization effect by the incorporated MeF byproducts.[21-23] The stabilization effect increases with the (molar) volume and lattice constant of the alkali metal fluorides.

The increased stabilization of carbyne chains against cross-linking is also reflected by the time dependence of the Raman spectra. Ageing (cross-linking) causes a decrease in the conjugation length and the relative carbyne content. The first effect is clearly demonstrated by the time dependence of the position for $\nu_{carbyne}$ (Figure 9). The decrease of the relative intensity between the carbyne line and the a-C line with time is less pronounced, but it can be noticed after several weeks of ageing. The ageing process is faster for C−LiF than for C−NaF and C−KF as can be seen from Figure 9. The same conclusion follows from previous studies of the time dependence of electronic conductivity[23] and electronic spectra.[21]

C. Resonance Raman Effect. Figures 6 and 8 illustrate a strong resonance enhancement of the Raman effect. The relative intensity of the carbyne line to the a-C line strongly increases with increasing laser energy. The a-C line can be used as a rough reference for the Raman intensity, because due to the extremely broadened electronic structure in a-C the intensity of the a-C line changes only weakly for laser energies below 3 eV.[45] A resonance for a-C does not exist until the laser energy has reached values between 4 and 6.5 eV. A similar argument can be used for the intensity ratio of the line $\nu_{carbyne}$ to the line of PTFE at 730 cm^{-1} since the laser energies used are in the sub-band gap region for PTFE. Thus, we can assume that the relative intensities of the carbyne line to the line of a-C or PTFE are roughly proportional to the Raman cross section of $\nu_{carbyne}$.

The intensity ratio of the carbyne line to the a-C line (and $\nu_{carbyne}$ to ν_{PTFE}) increases nonlinearly with the energy of the exciting laser. This increase runs parallel to the increase in the absorbance (see Figures 2 and 3), which proves that the broad feature in the absorption spectrum originates from the carbyne as it is was already mentioned in section V.A.

Not only the intensity but also the position of the carbyne line depends on the laser energy. The maximum of the carbyne line shifts more or less linearly to higher wavenumbers with increasing laser energy (Figure 7). This effect is much more pronounced for the carbyne line of C−LiF than for C−NaF and for C−KF. Akagi et al.[15] and Berdyugin et al.[31] reported values of about 60 and 55 cm^{-1}/eV, respectively, which are slightly larger as compared to our results. This dispersion effect in conjugated systems was studied in great detail in the past.[34,35,43,44,46] It originates from the correlation between conjugation length and the electronic structure and can be explained by a photoselective resonance process.[34,35] The dispersion is a quantitative measure for the conjugation length of a polymeric system. Since the dispersion decreases with increasing halogen radius, the degree of order and the conjugation length increase in the same way. A qualitative evaluation for the distribution function of the C≡C stretching mode will be presented in the next section.

D. Evaluation of the Conjugation Length Distribution Function. By applying the conjugation-length model for the C≡C stretching mode of the carbyne and using transition energies and matrix elements as presented in section IV, we have calculated the distribution function for the conjugation length. The conjugation-length model was originally developed for the explanation of the dispersion of the C=C stretching mode in conjugated polymers,[34,35] but we will show that it holds also for the C≡C stretching mode. By following the procedure described in refs 35 and 46 and using the A term of the Albrecht theory, one gets the expression for the Raman line shape

$$I(\nu,\epsilon) = C\sum_N P(N)|\alpha_{zz}(N)|^2\omega^3 L(\nu,N) \qquad (9)$$

with the transition polarizability α_{zz}

$$\alpha_{zz} = \sum_I M_{ge}{}^2 \sum_v \frac{\langle 0|v\rangle\langle v|1\rangle}{\Delta E + i\Gamma_e/2} \qquad (10)$$

and

$$\Delta E = E_I + h\omega v - \epsilon \qquad (11)$$

ν is the Raman frequency in wavenumbers, ϵ the energy of the exciting laser, C a constant, N the number of carbon atoms, $P(N)$ the distribution function, ω the frequency of the phonon, $L(\nu,N)$ a Lorentz function with full width half-maximum Γ_p, and E_I the pure electronic transition energy. The summation considers only diagonal transitions, because they are strongest. M_{ge} is the transition matrix element between the ground state and the excited state. The sum over v includes occupation numbers v from 0 to infinity. $\langle 0|v\rangle\langle v|1\rangle$ is the Franck−Condon integral, which is a function of the Franck−Condon coupling constant a_{FC}. In eq 10 a phenomenlogical full width half-maximum damping constant Γ_e describing the lifetime of the excited state was added.

For the frequency $\nu_{C=C}$ of the C=C stretching mode, the following relation is well known from conjugated polymers[35,43,46]

$$\nu_{C=C}(N) = \nu_{C=C}(\infty) + K/N \qquad (12)$$

where N is the number of carbon atoms and K is a constant. We have used an analogous equation for the conjugation length dependence of the C≡C stretching mode. $\nu_{C\equiv C}(\infty)$ and K were obtained by fitting eq 12 to the calculated frequencies of the Σ_g mode as presented in Figure 11. In this way we have obtained 1750 cm^{-1} for $\nu_{C\equiv C}(\infty)$ and 3980 cm^{-1} for K.

For the evaluation oligoynes up to 60 carbon atoms have been taken into consideration. A Gaussian function with an average conjugation length $\bar{N}$ and a half-width δN has been assumed for $P(N)$. To obtain a good fit of the calculated line positions to the experimental

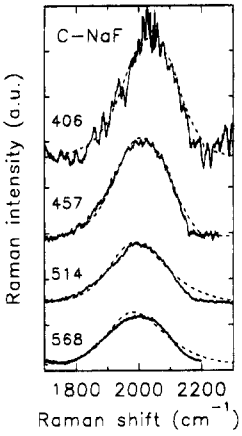

Figure 13. Experimental data (full lines) compared with calculated spectra (dashed lines) obtained from eq 9 with $\bar{N}$ = 12 and δN = 3 as the parameters of the Gaussian distribution function for C–NaF excited with 568, 514, 457, and 406 nm.

Raman spectra, the following parameters have been used: a_{FC} = 1.2, Γ_p = 120 cm^{-1}, and Γ_e = 0.5 eV.

A comparison between the experimental data and model calculation for the Raman spectra of C–NaF after excitation with 568, 514, 457, and 406 nm is shown in Figure 13. In this case an average conjugation length of 12 carbon atoms (=6 C≡C triple bonds) and a half-width δN = 3 have been used. The calculated curves fit well in position and shape to the experimental data, which demonstrates that the conjugation length model holds also for the dispersion effect of the C≡C stretching mode in carbynes.

Similar calculations have been performed for C–LiF and C–KF. For the former, best agreement with the experimental results was obtained with $\bar{N}$ = 8 and δN = 4 and for the latter with $\bar{N}$ = 14 and δN = 3.

VI. Conclusions

1. The composite "electrochemical carbon/alkali metal fluoride", C–MeF was prepared by a reaction of PTFE with alkali metal amalgams. This preparative method has previously been claimed as a potential source of the carbyne (polyyne) form of elemental carbon, but experimental evidences for this statement were, up to now, mostly speculative.

2. Raman spectra of the C–MeF composites indicate two broad lines centered at about 1300–1500 and 1950–2050 cm^{-1}. The second line is of considerable diagnostic significance, as it can be assigned to the C≡C–C stretching mode of a polyyne chain. The Raman spectra were interpreted in terms of a linear polyyne structure with $D_{\infty h}$ symmetry. The relative intensity of the polyyne line compared to the intensity of the line of amorphous carbon is the absolutely highest among all previously reported Raman spectra of a large variety of carbynoid species. The preparation of "electrochemical carbyne" with unusually high yield is thus demonstrated.

3. The intensity of the carbyne mode at around 2000 cm^{-1} increases, and the frequency of this line decreases as the cation becomes larger. Hence, the carbyne yield and the conjugation length increase in the same way. This behavior is a clear evidence that the individual carbyne chains can be stabilized by a spatial separation enabled by the MeF matrix. The higher is the atomic number of Me (molar volume of MeF), the better is the stabilization effect of the MeF matrix.

4. A quantum chemical calculation for the transition energies and matrix elements as a function of the chain length was presented and compared with experimental data obtained from oligoynes. The obtained values were used to interpret the dispersion of the C≡C stretching mode within the conjugation length model and to evaluate the conjugation length. The average conjugation length turned out to be about 8–14 carbon atoms.

5. The prepared carbyne chains tend to cross-link to graphene-like species during long-term ageing in vacuum. This results in a change of the optical spectrum from semiconductor-like to metal-like, an upshift of the Raman frequency of the carbyne line, and a (less pronounced) decrease in the relative intensity of this line. The cross-linking rate increases with decreasing atomic number of Me, which is another argument in favor of the hypothesis of carbyne stabilization by the MeF component (cf. (3) above).

Acknowledgment. This work was supported by the Osteuropa Förderung des BMfWF Project GZ 45.338/1-IV/6a/94 and by the Grant Agency of the Czech Republic, Contract No. 203/93/0251.

References and Notes

(1) Heimann, P. B.; Kleiman, J.; Salansky, N. M. *Carbon* **1984**, *22*, 147; *Nature* **1983**, *306*, 164.
(2) Kudryavtsev, Yu. P.; Evsyukov, S. E.; Babaev, V. G.; Guseva, M. B.; Khvostov, V. V.; Krechko, L. M. *Carbon* **1992**, *30*, 213.
(3) Smith, P. P. K.; Buseck, P. R. Science **1982**, *216*, 986; **1985** *229*, 486.
(4) Kertesz, M.; Koller, J.; Azman, A. *J. Chem. Phys.* **1978**, *68*, 2779.
(5) Karpfen, A. *J. Phys. C: Solid State Phys.* **1979**, *12*, 3227.
(6) Tanaka, K.; Okada, M.; Koike, T.; Yamabe, T. *Synth. Met.* **1989**, *31*, 181.
(7) Rice, M. J.; Phillpot, S. R.; Bishop, A. R.; Campbell, D. K. *Phys. Rev.* **1986**, *B34*, 4139; **1987**, *B36*, 1735.
(8) Springborg, M.; Drechsler, S. L.; Malek, J. *Phys. Rev.* **1990**, *B41*, 11954.
(9) Springborg, M.; Kavan, L. *Chem. Phys* **1992**, *168*, 249.
(10) Weltner, W.; van Zee, R. J. *Chem. Rev.* **1989**, *89*, 1713.
(11) (a) Shen, L. N.; Withey, P. A.; Graham, W. R. *J. Chem. Phys.* **1991**, *94*, 2395. (b) Martin, J. M.; Francois, J. P.; Gijbels, R. *J. Chem. Phys.* **1991**, *94*, 3753.
(12) Bjarnov, E.; Christensen, D. H.; Nielsen, O. F.; Aughdal, E.; Kloster-Jensen, E.; Rogstad, A. *Spectrochim. Acta* **1974**, *30A*, 1255.
(13) Korshak, V. V.; Kudravtsev, Yu. P.; Evsyukov, S. E.; Korshak, Yu. V.; Guseva, M. B.; Babaev, V. G.; Kostishko, B. M. *Dokl. Akad. Nauk SSSR* **1988**, *298*, 1421.
(14) Korshak, V. V.; Kudravtsev, Yu. P.; Evsyukov, S. E.; Korshak, Yu. V.; Khvostov, V. V.; Babaev, V. G.; Guseva, M. B. *Makromol. Chem., Rapid Commun.* **1988**, *9*, 135.
(15) Akagi, K.; Furukawa, Y.; Harada, I.; Nishiguchi, M.; Shirakawa, H. *Synth. Met.* **1987**, *17*, 557.
(16) Kavan, L. In *Electrochemical Carbonization of Fluoropolymers*; Thrower, P. A., Ed.; *Chemistry and Physics of Carbon*, Marcel Dekker: New York, 1991; Vol. 23, p 69.
(17) Costello, C. A.; McCarthy, T. J. *Macromolecules* **1987**, *20*, 2819.
(18) Iqbal, Z.; Ivory, D. M.; Szobota, J. S.; Elsenbaumer, R. L.; Baughman, R. H. *Macromolecules* **1986**, *19*, 2992.
(19) Jansta, J.; Dousek, F. P. *Carbon* **1980**, *18*, 433.
(20) Kijima, M.; Sakai, Y.; Shirakawa, H. In *Proc. Int. Conf. Sci. Technol. Synth. Met. 1994*, Seoul, Korea, *Synth. Met.*, to be published.
(21) Kavan, L.; Dousek, F. P. *Synth. Met.* **1993**, *58*, 63.
(22) Kavan, L.; Dousek, F. P.; Micka, K. *Solid State Ionics* **1990**, *38*, 109.
(23) Kavan, L.; Dousek, F. P.; Micka, K. *J. Phys. Chem.* **1990**, *94*, 5127.
(24) Červinka, L.; Dousek, F. P.; Jansta, J. *Philos. Mag.* **1985**, *B51*, 603.
(25) Dias, A. J.; McCarthy, T. J. *J. Polym. Sci., Polym. Chem. Ed.* **1985**, *23*, 1057.
(26) Kise, H.; Ogata, H. *J. Polym. Sci., Polym. Chem. Ed.* **1983**, *21*, 3443.

(27) Nakamizo, M.; Kammereck, R.; Walker, P. L. *Carbon* **1974**, *259*, 259.
(28) Tunistra, F.; Koenig, L. *J. Chem. Phys.* **1970**, *53*, 1126.
(29) Wright, R. B.; Varma, R.; Gruen, D. M. *J. Nucl. Mater.* **1976**, *63*, 415.
(30) Nishihara, H.; Harada, H.; Kaneko, S.; Tateishi, M.; Aramaki, M. *J. Chem. Soc., Faraday Trans.* **1991**, *87*, 1187.
(31) Berdyugin, V. V.; Kudryavtsev, Yu. P.; Evsyukov, S. E.; Korshak, Yu. V.; Shorygin, P. P.; Korshak, V. V. *Dokl. Akad. Nauk SSSR* **1989**, *305*, 362.
(32) Robertson, J. *Adv. Phys.* **1986**, *35*, 317.
(33) Li, F.; Lannin, J. S. *Appl. Phys. Lett.* **1992**, *61*, 2116.
(34) (a) Lefrant, S.; Lichtmann, L. S.; Temkin, H.; Fitchen, D. B. *Solid State Commun.* **1979**, *29*, 191. (b) Kuzmany, H. *Phys. Status Solidi* **1980**, *b97*, 521.
(35) Kuzmany, H. *Pure and Appl. Chem.* **1985**, *57*, 235.
(36) Longuett-Higgins, H. C.; Salem, L. *Proc. R. Soc. London* **1959**, *A251*, 172.
(37) Kürti, J.; Kuzmany, H. *Phys. Rev.* **1991**, *B44*, 597.
(38) Kürti, J.; Surján, P. R. *J. Math. Chem.* **1992**, *10*, 313.
(39) Kloster-Jensen, E. *Angew. Chem.* **1992**, *10*, 483.
(40) Eastmond, R.; Johnson, T. R.; Walton, D. R. M. *Tetrahedron* **1972**, *28*, 4601.
(41) Kavan, L.; Micka, K.; Kastner, J. *Synth. Met.* **1994**, *63*, 147.
(42) Knight, D. S.; White, W. B. *J. Mater. Res.* **1989**, *4*, 385.
(43) Kuzmany, H.; Kastner, J. In *Proceedings of the International IUPAC Symp. on Macromolecules 1992*; Kahovec, J., Ed.; VSP: Zeist, 1993; p 333.
(44) Zerbi, G.; Gussoni, M.; Castiglioni, C. In *Conjugated Polymers*; Bredas, J. L., Silbey, R., Eds.; Kluwer Academic Publishers: Amsterdam, 1991; p 435.
(45) Ramsteiner, M.; Wagner, J. *Appl. Phys. Lett.* **1987**, *51*, 1355.
(46) (a) Kastner, J.; Kuzmany, H.; Paloheimo, J.; Dyreklev, P. *Synth. Met.* **1993**, *55–57*, 558. (b) Kastner, J.; Pichler, T.; Kuzmany, H.; Curran, S.; Blau, W.; Weldon, D. N.; Delamesiere, M.; Draper, S.; Zandbergen, H. *Chem. Phys. Lett.* **1994**, *221*, 53.

MA941065N